TECHNICAL MEMORANDUM

276

Use of a neural network based longwave radiative transfer scheme in the ECMWF atmospheric model

F. Chevallier, J J. Morcrette,
F. Chéruy and N.A. Scott

Research Department

March 1999

European Centre for Medium-Range Weather Forecasts
Europäisches Zentrum für mittelfristige Wettervorhersage
Centre européen pour les prévisions météorologiques à moyen

Abstract

Although important uncertainties remain concerning the far wing absorbing line shapes and the effect of clouds, a high standard of accuracy has been achieved by the scattering line-by-line models for the modeling of the LW radiative transfer (e.g., Moncet and Clough, 1997). However, the definition of an approach that would enable computation times suitable for climate studies and a satisfactory accuracy, has proven to be a challenge for modellers. A fast radiative transfer model is tested at ECMWF: NeuroFlux (Chéruy *et al.*, 1996; Chevallier *et al.*, 1998b). It is based on an artificial neural network technique (the Multi-Layer Perceptron: Rumelhart *et al.*, 1986) used in conjunction with a classical cloud approximation (the multilayer grey body model: Washington and Williamson, 1977). The accuracy of the method is assessed through code-by-code comparisons, climate simulations and ten-day forecasts with the ECMWF model.

1 Introduction

Parametric representation, or parameterization, is used in numerical modeling of various atmospheric processes. It involves a statistical analysis, that enables the representation of the true processes by simpler parametric relations. Three purposes may motivate such an analysis: (i) getting a better understanding of the system (e.g., Bretherton et al., 1992), (ii) allowing a computation of the processes, that is faster than the exact formulation (as in numerous radiative transfer models - Goody and Yung, 1989), (iii) obtaining a simpler system without having to deal with the complicated details (as in precipitation schemes; e.g. Sundqvist, 1981).

The most accurate as well as the fastest longwave (LW) radiative transfer schemes include parameterized components. For instance, the current line-by-line computations take into account every absorption line from every absorbing gas, but usually do not exactly resolve the contribution of the line wings after a few tens of cm^{-1} off the centre of the lines. The absorption coefficients outside this interval are parameterized under the form of structureless continua, of which contribution to the radiation variations is essential (e.g., Clough *et al.*, 1992; Sinha and Harries, 1997). The high computational burden of the line-by-line codes prevents their use for most climatic studies and leads to the use of more heavily parameterized schemes. However, because a minimum accuracy is required, the resulting gain in computing time is still not sufficient and therefore many General Circulation Models (GCMs) reduce the frequency of radiation computations, compared to the other diabatic computations. This degrades the quality of the climate simulations (Wilson and Mitchell, 1986; Morcrette, 1999).

The interactions between LW radiation on the one hand and solid and liquid water on the other hand, add further difficulties to the atmospheric modeling. Indeed, the computational burden of the most accurate approaches limits their applicability, and furthermore, all the variables that they need in input are seldom available. This is obvious in the GCMs, where the subgrid processes, like the distribution of the cloud particles in a vertical layer, are crudely treated. Some approximations are necessary to deal with this lack of knowledge.

The parameterizations, the temporal sampling and the approximations lead to high uncertainties in the climate studies and in weather forecasts. Therefore, improvement of the LW radiative codes is a key objective for atmospheric modeling. An original approach has been initiated at LMD (Chéruy *et al.*, 1996; Chevallier *et al.*, 1998b). It makes use of an artificial neural network technique: the multilayer perceptron (MLP) as defined by Rumelhart *et al.* (1986).

It has been carried out in a highly parameterized scheme called NeuroFlux, that combines the MLP with a classical cloud approximation: the multilayer grey body model (Washington and Williamson, 1977). All the parameters in NeuroFlux, several tens of thousands, are inferred from a series of learning databanks during supervised learning phases (Chevallier *et al.*, 1998b). The neural network-based method enables fast computing times: on a 19 vertical layer-grid, a gain in computation time of at least one order of magnitude compared to the operational code at ECMWF (European Centre for Medium-Range Weather Forecasts) has been recorded. Concerning the accuracy, satisfactory results of code-by-code comparisons between NeuroFlux and other radiative transfer models, were obtained (Chevallier *et al.*, 1998b). Preliminary tests of NeuroFlux in the LMD GCM (Sadourny and Laval, 1984) led to further developments of the method (Chevallier *et al.*, 1998a, Chevallier *et al.*, 1999).

This paper presents the results of the testing of NeuroFlux in the ECMWF GCM in its 31 vertical layer configuration. It is is structured as follows. Section 2 describes the neural network-based radiative transfer model. Section 3 presents its instantaneous error through code-by-code comparisons with the ECMWF operational scheme (Morcrette, 1991; Zhong and Haigh, 1995). The impact of NeuroFLux on climate simulation is evaluated in section 4. Comparisons of the simulations with ECMWF analyses of the atmosphere and with observations are used in section 5 to have a quantitative estimation of the uncertainty introduced. Section 6 contains the conclusions.

2 Principles of NeuroFlux

2.1 The multilayer perceptron

A MLP (Rumelhart *et al.*, 1986) is an artificial neural network, that realizes a non-linear application from an input space to an output space. The information is propagated from its inputs to its outputs by non-linear projections on successive spaces, that transform and filter it. Each variable of the various spaces is computed by a non-linear (sigmoidal) transformation of a weighted sum of the variables from the previous space. The weights of the sums are the parameters of the MLP. They are inferred once and for all during a supervised learning. A non-linear regression, based on a gradient descent, iteratively adapts the parameters of the projections, so that together, they achieve an optimal transformation from the inputs of the learning dataset to its outputs. It should be noted that, due to this statistical technique, the choice of the learning dataset is of crucial importance for the accuracy of the multilayer perceptron parameterization. The gradient descent technique requires the sigmoidal function to be differentiable. Furthermore, the existence of horizontal asymptotes are important to avoid the propagation of high values in the MLP. In the following, the sigmoidal functions are the widely used hyperbolic tangent.

The simple structure of the MLP enables fast computing time for the MLP relatively to its number of parameters. Therefore, the MLP is an interesting tool for parameterization. The MLP could be used at various stages in parameterized radiative computations, for example for the computation of transmissions or for the whole flux computations. In NeuroFlux, the MLP is combined with an other parameterized scheme, the multilayer grey body model, to compute the fluxes.

2.2 The multilayer grey body model

The multilayer grey body model does not include any artificial neural network, but rather relies on a probabilistic approach, common to many LW radiation codes, to treat radiation through a pile of overlapping cloudy layers. Assuming the hypothesis of a plane parallel atmosphere, the atmosphere is divided into a stack of N horizontal layers, from the surface to the top of the atmosphere (TOA). In the following, the bottom layer is layer 1, the top layer is layer N. Following the multilayer grey body approach, clouds are introduced as grey bodies. Their contribution to the fluxes is determined by their horizontal coverage n_i and their LW emissivity ϵ_i, in each vertical layer i of the model (Washington and Williamson 1977). ϵ_i can be derived from the cloud liquid (or ice) water path l_i by the following equation:

$$\epsilon_i = 1 - e^{-kl_i} \tag{1}$$

where k is the longwave extinction coefficient whose value varies according to the nature (liquid or ice) of the cloud (Ebert and Curry, 1992). Equation (1) is a simple parameterization of the scattering effect in the clouds. As its introduction in GCMs is straight-forward, it is used in most of the present longwave fast schemes.

This approach leads to the following expressions for the upward and downward LW radiative fluxes (e.g., Harshvardhan *et al.*, 1987):

$$F^{\uparrow}(P_i) = (1 - C_{H,i})F^{\uparrow}_H(P_i) + \sum_{k=0}^{H-1}(1 - C_{k,i})F^{\uparrow}_k(P_i) \prod_{l=k+1}^{H} C_{l,i} \tag{2}$$

$$F^{\downarrow}(P_i) = (1 - C_{i,N})F^{\downarrow}_{J+1}(P_i) + \sum_{k=i+1}^{J+1}(1 - C_{k,i})F^{\downarrow}_k(P_i) \prod_{l=k-1}^{J} C_{l,i} \tag{3}$$

H (resp. J) is the index of the highest cloudy layer below (resp. above) the level of calculation, $C_{k,i}$ is the probability of a cloudy line of sight between the levels k and i, $F^{\uparrow}_k(P_i)$ (resp. $F^{\downarrow}_k(P_i)$) the upward (resp. downward) flux at pressure level P_i, if the only cloud in the atmosphere was a black body in layer k. With this formalism $F^{\uparrow}_0$ and $F^{\downarrow}_0$ correspond to the fluxes in the absence of clouds. The $F^{\uparrow}_k$'s and the $F^{\downarrow}_k$'s, $k \geq 0$, all are quantities of the form:

$$Q(P, P_b) = \int_{-1}^{+1} \mu \, d\mu \int_{\nu} d\nu \;\; B_{\nu}(T_{P_b}) \, \tau_{\nu}(P_b, P, \mu) + \int_{P_b}^{P} B_{\nu}(T_{P'}) \, \frac{\partial \tau_{\nu}(P', P, \mu)}{\partial P'} dP' \tag{4}$$

where P and P_b are pressure levels at the boundary of an atmospheric layer, ν is the frequency, μ the cosine of the zenith angle, $B_{\nu}(T_P)$ the Planck function at temperature T_P, $\tau_{\nu}(P, P', \mu)$ the monochromatic flux transmittance for isotropic radiation.

The $C_{k,i}$'s in equations (2) and (3), are called *cloud fractional coverages*. They are functions of the n's and of the ϵ's and depend on the way the cloudy layers overlap. Various overlapping hypotheses can be taken into account according to the vertical structure of the clouds: for instance the maximum-random overlap (Geleyn and Hollingsworth, 1979) currently used at ECMWF.

According to equations (2) and (3), the LW fluxes in the presence of multilayer grey bodies, $F^{\uparrow}$ and $F^{\downarrow}$, can be deduced from the clear sky fluxes, $F_0^{\uparrow}$ and $F_0^{\downarrow}$, and from the fluxes in presence of single layered black clouds, $F_k^{\uparrow}$ and $F_k^{\downarrow}$, $k > 0$.

2.3 The algorithm

In NeuroFlux, the computation of the $F_k^{\uparrow}$'s and of the $F_k^{\downarrow}$'s, $k \geq 0$, in equations (2) and (3), is achieved by a series of MLPs, rather than by a physically explicit scheme. Two neural networks (respectively NN-Clr$^{\uparrow}$ and NN-Clr$^{\downarrow}$) compute the clear sky part of the LW fluxes (respectively $F_0^{\uparrow}$ and $F_0^{\downarrow}$). Then a battery of $2 \times N$ neural networks (the NN-Cld's) computes the contribution of every cloudy layer, $F_k^{\uparrow}$ and $F_k^{\downarrow}$, with $k > 0$. Each neural network among the NN-Cld's is dedicated to the calculation of the fluxes, either upward or downward, in the presence of a single black cloud in a specified layer k. The overall fluxes $F^{\uparrow}$ and $F^{\downarrow}$ are then computed according to equations (2) and (3). Thus, NeuroFlux includes $(2 + 2 \times N)$ neural networks.

NeuroFlux is currently defined in such a way that each version of the scheme is dedicated to a specified vertical discretization. If the vertical discretization is changed, the training process on the new system has to be conducted again. In this study, the vertical discretization is defined from the ECMWF GCM with 31 layers: the temperature, water vapour and ozone concentrations, as well as the cloudiness effective emissivity, are defined in the middle of these. The mean CO_2 concentration and relevant characteristics of the surface, namely its temperature, pressure and mean LW emissivity in the window region (800-1250 cm^{-1}), are also inputs to the model. The concentration of the minor gases (N_2O and CH_4 for example) and of the aerosols are set to the mean current level.

2.4 The learning datasets

The choice of the learning datasets has been the most involving part in the development of the neural network-based radiative transfer model. Indeed, because of the high level of parameterization in NeuroFlux, the accuracy of the scheme dramatically depends on their statistical characteristics. The latest learning datasets are based on a 6,000 sounding set: the latter one comes from the sampling of 1,350,000 atmospheric situations from the ECMWF short-range forecasts. The method is detailed in (Chevallier *et al.*, 1999). The 6,000 soundings are represented by temperature and water vapour profiles. Among the variables that are necessary for the radiative computations, some are not archived in the set: the ozone and cloudiness profiles, the mean CO_2 concentration and the surface characteristics. The ozone profiles have been added from a climatology dependent on season and latitude (Fortuin and Langematz, 1994). The mean CO_2 concentration, the surface temperature and LW emissivity in the window region have been introduced by random drawings between selected boundaries, insuring regular repartitions desirable for the MLP learnings. As the NN-Clr's and the NN-Cld's differ altogether in the position of the cloud layer among the 31 possible, the cloudiness simply derives from the learning dataset considered: the learning dataset of the NN-Clr's include the 6,000 soundings without any cloud, whereas the other learning datasets include the same 6,000 soundings, associated with the systematic presence of a black body in a particular layer. Due to these techniques, the learning sets contain atmospheric situations that may never be observed in the

atmosphere: they are not only compilations of real atmospheric situations, but are devoted to teach the networks the computation of LW radiative fluxes from thermodynamic profiles. For this purpose, it is suitable that a physical phenomenon, like the presence of a cloud in the atmospheric layers, has a regular more than a realistic distribution in the learning datasets.

In the present study, the ECMWF operational LW code (Morcrette, 1991; Zhong and Haigh, 1995) was used to compute the radiative characteristics of these soundings (the LW fluxes from equations (2) and (3)). In the following, it will be referred to as "EC-OPE". Any other LW radiative transfer model can be chosen, including a line-by-line code: the learning phases are the most time-consuming step of NeuroFlux, but they are run only once. The routine utilisation of NeuroFlux is computationally cheap.

2.5 Validation method

A new version of NeuroFlux has been set up with these learning datasets. Compared to EC-OPE, it is seven times faster (mean computing time recorded on a Fujitsu VPP700 in the framework of a ten-day forecast). If NeuroFlux was a perfect simulator, the result of its computations would be identical to the result of EC-OPE computations. In fact, the neural network parameterization introduced a small uncertainty in the fluxes and cooling rates. This has been studied from three points of view: in terms of errors in cooling rates and fluxes, in terms of long-term (four months) climate simulations, and in terms of forecast accuracy. For the last two points, the methodology follows the approach of Morcrette *et al.* (1998) who studied the impact of the change of radiative transfer model to RRTM (Rapid Radiative Transfer Model; Mlawer *et al.*, 1997) in the ECMWF GCM.

3 Validation of NeuroFlux through code-by-code comparisons

In this section, a code-by-code comparison is presented. It is based on the ECMWF forecast archive of profiles. Radiative fluxes obtained by using NeuroFlux and by using EC-OPE have been compared for the whole globe. Global archives from the first of June 1998 for the four synoptic times (00, 06, 12 and 18 UTC) and at operational resolution 0.5625° × 0.5625° were taken into account in the statistics: 800,000 atmospheric situations. Results are presented in three latitude classes. The tropical class covers the 30°N - 30°S region. The mid-latitude class covers the 60°N - 30°N region and the symmetrical band in the southern hemisphere. The polar class covers the 30° bands surrounding the two poles. For the three latitude classes, the biases and standard deviations of the differences between the radiative calculations of NeuroFlux and those of EC-OPE were computed, as well as the maximum absolute differences. Results for LW cooling rates are shown on Figure 1.

The standard deviations and the absolute biases respectively are less than 0.4 $K.d^{-1}$ and 0.2 $K.d^{-1}$, except in the lower layer where the standard deviations is around 0.3 $K.d^{-1}$ and the bias around 1.4 $K.d^{-1}$. The maximum error reaches 10 $K.d^{-1}$. The higher standard deviations in the lower layer are discussed from the neural network point of view by Chevallier *et al.* (1999). Their impact on atmosphere simulation is examined in the following. Similar statistics are presented for the outgoing longwave radiation (OLR) and the surface net flux in Table 1.

Standard deviations and absolute biases respectively are less than 1.7 $W.m^{-2}$ and 0.8 $W.m^{-2}$. Maximum values reach 7 $W.m^{-2}$ for the OLR and 9 $W.m^{-2}$ for the surface net flux. Very similar results are shown in Chevallier *et al.* (1999) for analysis archives, as well as for forecast data.

To our knowledge, no radiative transfer has been validated with reference computations on such a high number of soundings. In particular, the maximum errors performed by ECOPE, with reference to the real values, are not known. They are expected to be larger in cloudy sky, because of the weakness of the cloud radiative transfer parameterization, shared by most of today's radiative transfer codes. Nevertheless, the availability of such an exhaustive documentation of the errors of NeuroFlux leads to strong questions about their impact on GCM simulations. This is explored in details in the following sections.

4 Validation of NeuroFlux through climate simulations

4.1 Methodology

The assessment of the impact of NeuroFlux in climate simulations has been performed as follows. An ensemble of 10 members of 4-month forecasts were run with initial dates between 21/04/87 and 30/04/87. Cycle 18r5 of the ECMWF model has been used, with a T63 truncature, equivalent to a 1.875° × 1.875° horizontal resolution. T63 is the usual configuration at ECMWF for extended-range studies, even though operational forecasts use a smaller grid (0.5625° × 0.5625°). Indeed, Tibaldi et al. (1990) showed that T63 was sufficiently fine for climate studies. The shortwave radiation transfer in the GCM is based on Fouquart and Bonnel (1980) (Morcrette, 1991). Since the atmosphere has a strong chaotic behaviour, the simulations have been studied as means over the 3-month period between 01/06/87 and 30/08/87 and over the 10-member ensemble.

4.2 LW fluxes at the boundaries and cloudiness

For the three-month average, the impact of NeuroFlux on the clear sky OLR (figure 2) is mostly under 2 $W.m^{-2}$, which is comparable to the uncertainty in the instantaneous OLRs from NeuroFlux (1 $W.m^{-2}$, see Table 1). Limited areas display stronger impact, but still under 5 $W.m^{-2}$. By comparison, the recent change of the surface emissivity in the LW window region (800-1250 cm^{-1}) from 0.99 to 0.93 for the desert regions in the ECMWF GCM (Gregory et al., 1998) affected the clear sky OLR by more than 5 $W.m^{-2}$ over the corresponding regions in the same conditions of experiment.

The differences are stronger when the clouds are taken into account in the OLR (figure 3), though remaining under 14 $W.m^{-2}$. This is not surprising since cloud models use step functions: small differences in temperature or water vapour can make clouds appear or disappear. Indeed, as shown on figure 4, the simulations using NeuroFlux are marked by a small decrease (between 0.01 and 0.03 on an average) of high level cloud cover in the Inter-Tropical Convergence Zone (ITCZ). This is associated with the increase of full sky OLR in the same region on an average (figure 3). As far as the other latitudes are concerned, the impact of NeuroFlux on cloud cover appears to be rather limited, to 0.01, with a maximum at 0.06. The differences for the surface

net flux, shown on figure 5, corroborates the results concerning the OLR.

4.3 Impact of the temporal resolution of the radiative computations

One of the main motivations in the development of NeuroFlux has been the interest in fast codes that could resolve the diurnal cycle better than the existing codes. As an example, in the ECMWF model, the full radiation code is called every three hours whereas the "time-step" for the rest of the model varies from 20 minutes for the operational model to one hour for the seasonal simulations. Morcrette (1999) showed that the main impact of this reduced computation frequency is a decrease of the convection and therefore of the high level cloudiness in the tropics. Climate simulations yet incorporate this artificial signal, even though this missing cloudiness tends to warm the stratosphere and cool the troposphere, and therefore degrades the climate sensitivity studies.

The question arises if the accuracy of Neuroflux is enough to restore the right climatic signal if Neuroflux is called more often in the simulations. In order to assess this question, the following experiment has been conducted. The ensemble simulations using either NeuroFlux or EC-OPE have been repeated with a time-step of 60 minutes for the radiation instead of three hours. Because NeuroFlux is seven times faster than EC-OPE, even this configuration using NeuroFlux is cheaper than the current configuration with EC-OPE and a three-hour time step. Figure 6 shows some differences between the configurations: when only the time-step is changed, with either NeuroFlux (figure 6a) or EC-OPE (figure 6b). As said before, the main signal induced by the time-step change is the high level cloudiness in the ITCZ. This signal is correctly captured by NeuroFlux. The uncertainty introduced by NeuroFlux in the cloud cover simulations is far smaller than that one induced by the reduced frequency of radiative computation in the climate simulations.

5 Impact of NeuroFlux on forecast accuracy

The evaluation of the quality of the simulations using NeuroFlux has also been evaluated by comparison with analyses of the atmosphere, expressed into objective scores. Two ensembles of twelve ten-day forecasts, starting on the 15th of each month from 15 April 1997 to 15 March 1998, have been gathered. The LW model, either NeuroFlux or EC-OPE, is the only difference between the sets. The horizontal resolution corresponds to a T213 truncature. Figure 7 presents the scores for the Northern hemisphere, defined as the region between 20°N and 90°N. Similar results have been obtained for the tropical band, and the Southern hemisphere. The impact of NeuroFlux appears to be negligible on the 500 hPa and 1000 hPa geopotentials, as well as on the temperature at 850 hPa, 500 hPa, 200 hPa and 50 hPa. For instance, the mean differences for the temperature are of the order of a hundredth of degree without exhibiting any significant trend.

Because the instantaneous error of NeuroFlux is higher in the lower layer (figure 1), a special attention has been paid to the quality of the 2-meter temperature forecast. This study is illustrated here with the 10-day forecast for the 25th of January 1998. Figures 8 and 9 display the difference between the two forecasts and the corresponding observations over Europe at 12 UTC. Biases, around 1.4 K, and standard deviation, around 3.5 K, are similar for

the two forecasts. In this particular case, NeuroFlux even performs slightly better. This result illustrates that the uncertainty introduced by NeuroFlux in the GCM simulation, of the order of 1 K or less for the 10-day forecast of the 2-meter temperature, does not make the simulation diverge from the real atmosphere, as far as the 2-meter temperature is concerned. It corroborates from a different point of view the study of the scores, that relies on zonal means and on a statistical ensemble.

6 Conclusions

The structure of the ECMWF operational LW radiative transfer code, based on the work of Morcrette (1984, 1991), has proven to be suitable for incorporating recent important developments in radiative transfer, such as those on water vapour continuum (Zhong and Haigh, 1995) and cloudiness (Raïsänen, 1998). However, like the other radiative transfer models used in GCMs, because of computational costs, it is still necessary to apply both a spatial and a temporal sampling in the usual climate simulations. This code has been parameterized through the neural network-based approach developed by Chéruy et al. (1996) and Chevallier et al. (1998b). This new radiative transfer code, called NeuroFlux, was shown to be seven times faster than the original code. The evaluation of the error introduced in the climate simulations by this approach, compared to the original code, is a painstaking work because of the numerous possible points of view for its validation. This paper illustrates the chosen validation methodology. Firstly, code-by-code comparisons have quantified the instantaneous error of NeuroFlux. Then the impact of this error on climate simulation has been estimated through four-month simulations, with emphasis on longwave boundary fluxes and cloudiness. Finally, the qualitative estimation of this error has been made by comparisons of ten-day forecasts with ECMWF analyses of geopotential and atmospheric temperature on the one side, and surface observations of 2-meter temperature on the other one. Through these various studies, the accuracy of NeuroFlux appears to be comparable to the accuracy of the original scheme, with a negligible impact on the simulations. The use of NeuroFlux in a 6-day forecast-assimilation process has confirmed the various results reported here: the departure of the background forecasts as well as of the analyses from the observations appear to be the same with NeuroFlux than with the operational configuration (result not shown).

The potential of the neural network-based approach has not yet been fully used at ECMWF. In particular, as shown by Chevallier et al. (1998b), the use of a more accurate radiative transfer code in the learning phase, like a line-by-line model or RRTM for instance (Mlawer et al., 1997), would reduce the current biases of EC-OPE in the clear sky contribution to the fluxes, while keeping the same reduced computational burden. The various tests that we performed tend to show that the standard deviations of NeuroFlux compared to the original code, whatever it is, can not be further reduced. Though, they do not appear to affect the simulations. The cloud parameterization, that is classically formulated in NeuroFlux (Washington and Williamson, 1977), obviously brings much more uncertainty to the code, although quantifying this is rather difficult, due to the lack of observations of radiative cooling rates.

Even without any further improvement, NeuroFlux appears to be suitable for two main applications in atmospheric studies. The first one is the reduction of the cost of the radiative computations in atmospheric models, like those used in ensemble predictions, coupled atmosphere-ocean simulations, or four dimensional variational assimilation, for extended use of

these. The second application is the improvement of the climate simulations if the computational savings are used to increase the radiative computation frequency in the GCMs. Indeed, we showed that the uncertainty introduced by NeuroFlux in the simulations is negligible compared to the effect of an increase of the radiation time-step in the GCMs, as studied by Wilson and Mitchell (1988) and Morcrette (1999).

Acknowledgements

Authors wish to thank M. Miller and A. Beljaars for careful review of the manuscript.

References

Bretherton, C. S., C. Smith, and J. M. Wallace, 1992: An intercomparison of methods for finding coupled patterns in climate data. *J. Climate*, 5, 541-560.

Chéruy, F., F. Chevallier, J.-J. Morcrette, N.A. Scott, and A. Chédin, 1996 : Une méthode utilisant les techniques neuronales pour le calcul rapide de la distribution verticale du bilan radiatif thermique terrestre. *C. R. Acad. Sci. Paris*, 322:IIb, 665-672, in French.

Chevallier, F., A. Chédin, F. Chéruy, J.-J. Morcrette, and N. A. Scott, 1999: A TIGR-like atmospheric profile database for accurate radiative flux computation. Submitted to *Quart. J. Roy. Meteor. Soc.*.

Chevallier, F., F. Chéruy, Z. X. Li, and N. A. Scott, 1998a: A fast and accurate neural network-based computation of longwave radiative budget: application in a GCM. In *Proc. of the Am. Meteor. Soc.*, Paris, France, in press.

Chevallier, F., F. Chéruy, N. A. Scott, and A. Chédin, 1998b: A neural network approach for a fast and accurate computation of longwave radiative budget. *J. Appl. Meteor., 37:11,* 1385-1397, 1998.

Clough, S. A., M. J. Iacono, and J.-L. Moncet, 1992: Line-by-line calculations of atmospheric fluxes and cooling rates : application to water vapor. *J. Geophys. Res.*, 97:D14, 15761-15785.

Ebert, E. E., and J. A. Curry, 1992: A parametrisation of ice cloud optical properties for climate models, *J. Geophys. Res.*, 97D, 3831-3836.

Fortuin, J. P. F. and Langematz, U., 1994: An update on the global ozone climatology and on concurrent ozone and temperature trends. *Proceedings SPIE*, 2311, 207-216.

Fouquart, Y. and B. Bonnel, 1980: Computation of solar heating of the Earth's atmosphere: a new parameterization. *Beitr. Phys. Atmosph.*, 53, 35-62.

Geleyn, J. F. and T. Hollingsworth, 1979: An economical and analytical method for the computation of the interaction between scattering and line absorption of radiation. *Beitr. Phys. Atmosph.*, 52, 1-16.

Goody, R. M. and Y. L. Yung, 1989: Atmospheric radiation. Theoretical basis. Oxford Unversity Press, 519 p.

Gregory, D., J.-J. Morcrette, C. Jakob, and A. Beljaars, 1998: Introduction of revised radiation, convection, cloud and vertical diffusion schemes into Cy18r3 of the ECMWF integrated forecasting system. ECMWF Technical Memorandum No. 254 [available from ECMWF, Shinfield Park, Reading, Berks. RG2 9AX, UK].

Harshvardhan, D., Randall, A., Corsetti, T.G., 1987 : A fast radiation parameterization for atmospheric circulation models. *J. Geophys. Res.*, 92, 1009-1016.

Mlawer, E. J., S. J. Taubman, P. D. Brown, M. J. Iacono, and S. A. Clough, 1997: Radiative transfer for inhomogeneous atmospheres : RRTM, a validated correlated-k model for the longwave. *J. Geophys. Res.*, 102, 16663-16682.

Moncet, J.-L. and S. A. Clough, 1997: Accelerated monochromatic radiative transfer for scattering atmospheres: application of a new model to spectral radiance observations. *J. Geophys. Res., 102:D18, 21,853-21,866.*

Morcrette, J.-J., 1984 : Sur la paramétrisation du rayonnement dans les modèles de circulation générale atmosphérique. Ph.D. Thesis, University of Lille.

Morcrette, J.-J., 1991 : Radiation and Cloud Radiative Properties in the European Centre for Medium Range Weather Forecasts forecasting system. *J. Geophys. Res.*, 96:D5, 121-9132.

Morcrette, J.-J., S. A. Clough, E. J. Mlawer, and M. J. Iacono, 1998: Impact of a validated radiative transfer scheme, RRTM, on the ECMWF model climate and 10-day forecasts. ECMWF Technical Memorandum No. 252 [available from ECMWF, Shinfield Park, Reading, Berks. RG2 9AX, UK].

Morcrette, J.-J., 1999: On the Effects of the Temporal and Spatial Sampling of Radiation Fields on the ECMWF Forecasts and Analyses. Mon. Wea. Rev., submitted.

Räisänen, P., 1998: Effective longwave cloud fraction and maximum-random overlap clouds - a problem and a solution. Accepted for publication in the *Mon. Wea. Rev.*

Rumelhart, D.E., Hinton, G.E., Williams, R.J., 1986 : Learning internal representations by error propagation, Parallel distributed processing: Explorations in the macrostructure of cognition 1, Rumelhart and McClelland eds, MIT Press.

Sadourny, R. and Laval, K., 1984 : January and July performances of the LMD general circulation model. New perspectives in climate modelling, Berger and Nicolis Eds., Elsevier, 173-198.

Sinha, A., and J. E., Harries, 1997: The Earth's clear-sky radiation budget and water vapor absorption in the far infrared. *J. Clim., 10, 1601-1614.*

Sundquist, H., 1981: Parameterization of condensation and associated clouds in models for weather prediction and general circulation simulation. Tellus, 33, 344-355.

Tibaldi, S., T. N. Palmer, Č. Branković, F. Molteni, and U. Cubasch, 1990: Extended-range predictions with ECMWF models: influence of horizontal resolution on systematic errors and forecast skill. operational model integrations. *Quart. J. Roy. Meteor. Soc.*, 116, 835-866.

Washington, W.M. and D.L. Williamson, 1977 : A description of the NCAR GCM's in General circulation models of the atmosphere. Method in Computational Physics, J. Chang. Ed., 17, Academic Press, 111-172.

Wilson, C. A. and Mitchell, J. F. B., 1986 : Diurnal variation and cloud in General Circulation Model. *Quart. J. Roy. Meteor. Soc.*, 112, 347-369.

Zhong, W., and J. D. Haigh, 1995: Improved broadband emisivity parameterization for water vapor cooling rate calculations. *J. Atmos. Sci.*, 52:1, 124-138.

(a)

	polar			mid-latitude			tropical		
	m	σ	M	m	σ	M	m	σ	M
NeuroFlux - EC-OPE	0.28	0.85	4.84	-0.06	0.77	4.85	-0.16	0.89	7.17

(b)

	polar			mid-latitude			tropical		
	m	σ	M	m	σ	M	m	σ	M
NeuroFlux - EC-OPE	0.76	1.72	8.07	0.16	1.06	6.83	-0.12	0.88	9.34

Table 1: Mean (m), standard deviation (σ) and absolute maximum difference (M) of the comparisons between NeuroFlux and EC-OPE for the computation of the OLR (a), and the net flux at the surface (b) (fluxes from NeuroFlux minus fluxes from EC-OPE). ECMWF 6-hour forecasts, L31 T319. 1^{st} June 1998, 00, 06, 12 and 18 UTC. Fluxes in $W.m^{-2}$. Results are shown in three latitude classes.

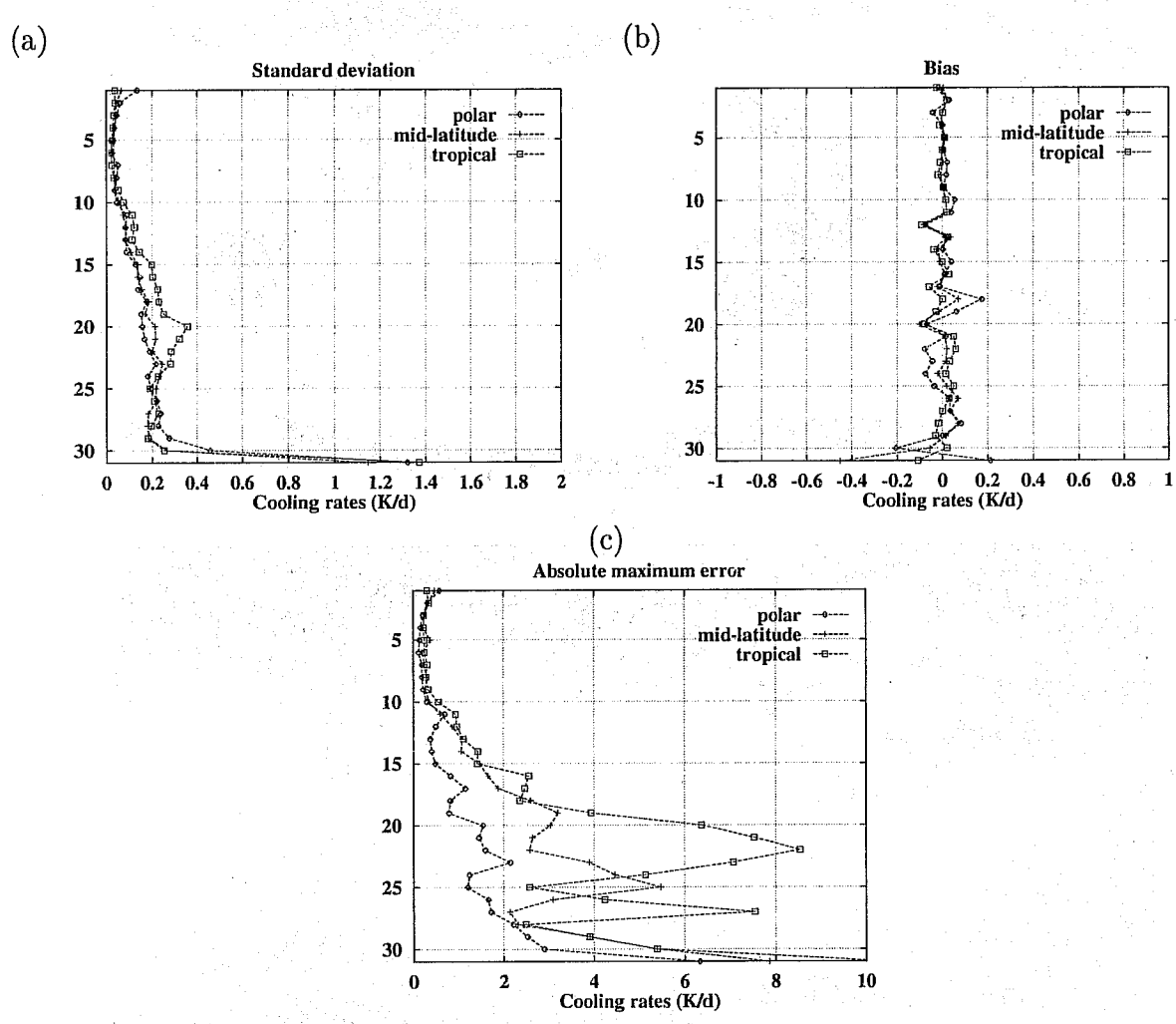

Figure 1: Comparison between the computations of NeuroFlux and those of EC-OPE: cooling rates from NeuroFlux minus cooling rates from EC-OPE, in $K.d^{-1}$. ECMWF 6-hour forecasts, L31 T319. 1^{st} June 1998, 00, 06, 12 and 18 UTC. Results are shown in three latitude classes. Figures (a) and (b) respectively show the biases and standard deviations in each latitude class. The maximum absolute differences are plotted on figure (c).

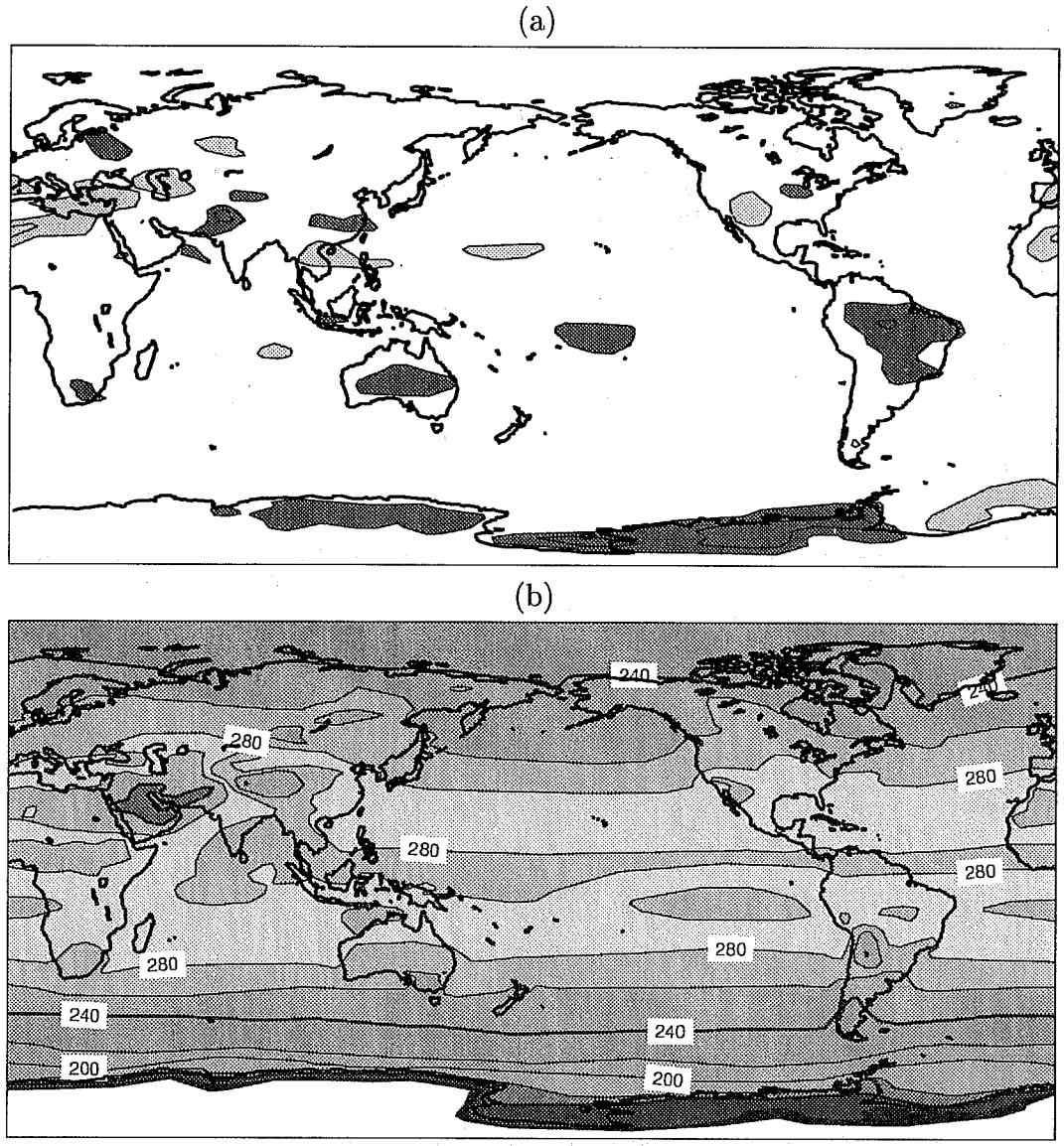

Figure 2: Top panel is the difference between the clear sky OLR averaged over ten simulations and over three months, with the ECMWF GCM using either NeuroFlux or EC-OPE (simulations using NeuroFlux minus simulations using EC-OPE). The OLR is in $W.m^{-2}$. Contours every 2 $W.m^{-2}$. Negative values less than -2 $W.m^{-2}$ are dark-shaded, positive values greater than 2 $W.m^{-2}$ are light-shaded. The values for EC-OPE are shown on the lower panel. Contours every 20 $W.m^{-2}$.

(a)

(b)

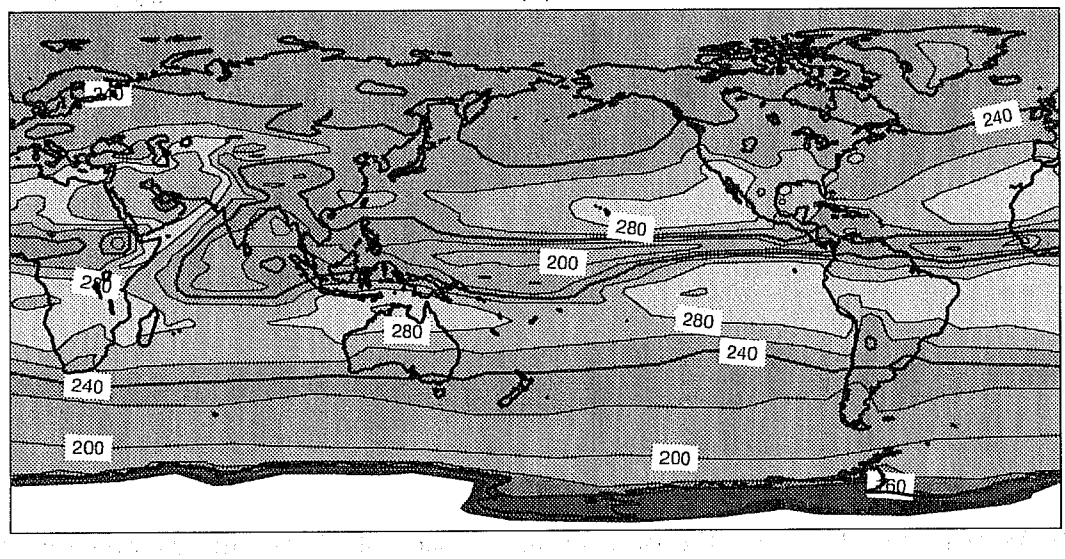

Figure 3: As in Figure 3, but for the full sky OLR, in $W.m^{-2}$.

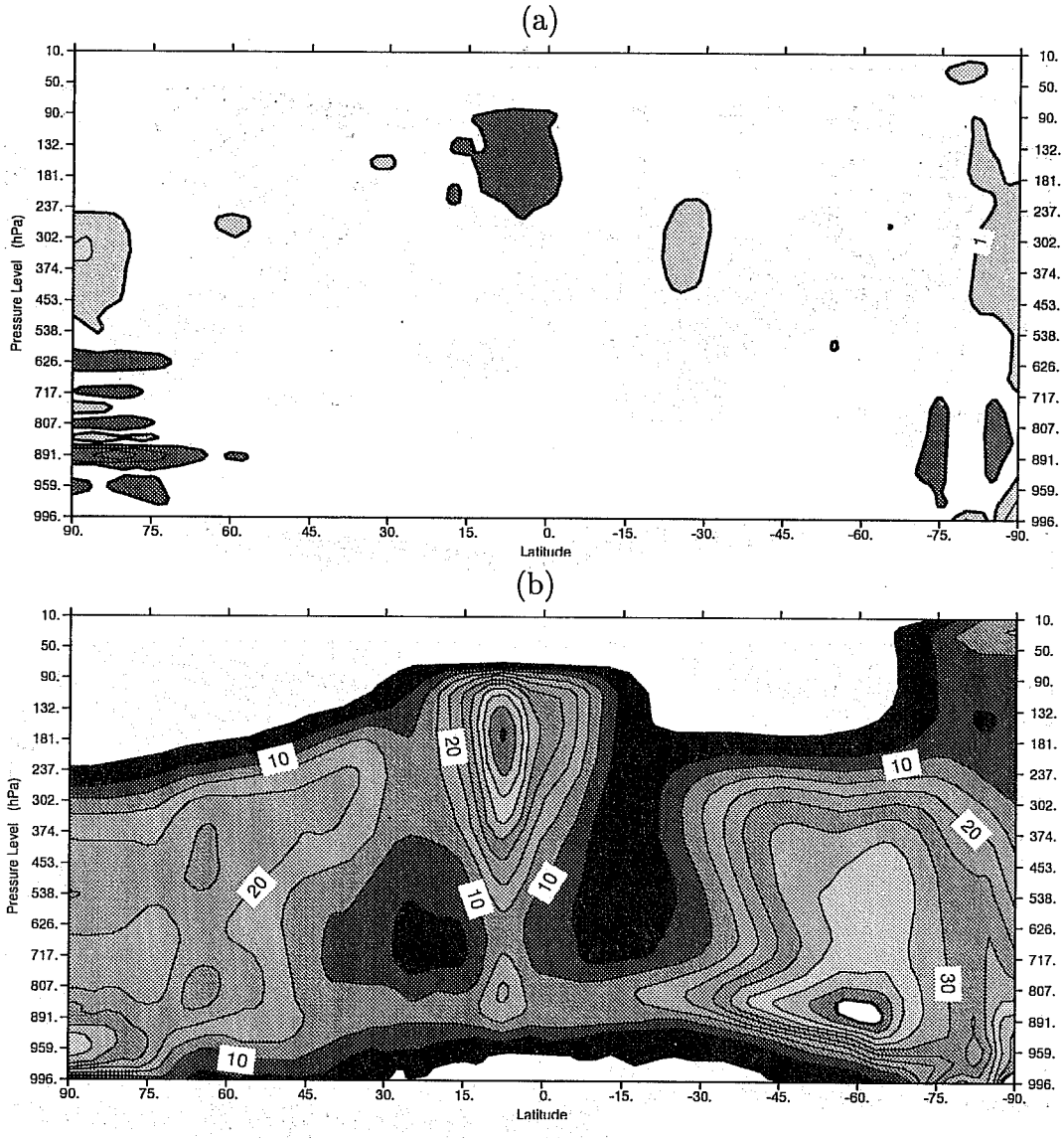

Figure 4: As in Figure 3, but for the vertical distribution of the zonally averaged cloud cover, in %. Top panel: contours every 2%; negative values less than -1% are dark-shaded, positive values greater than 1% are light-shaded. Bottom panel: contours every 5%.

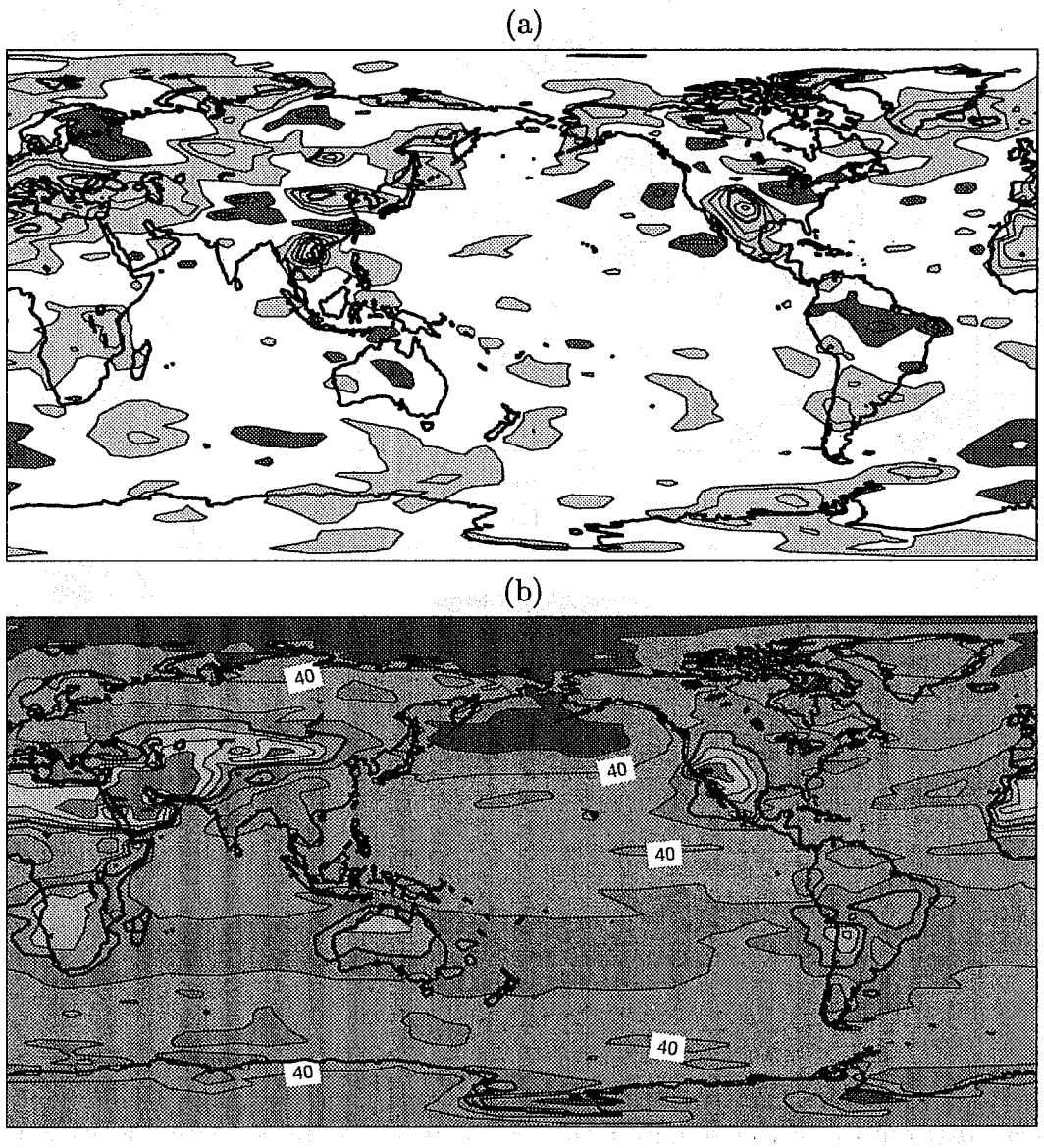

Figure 5: As in Figure 3, but for the net flux at the surface, in $W.m^{-2}$.

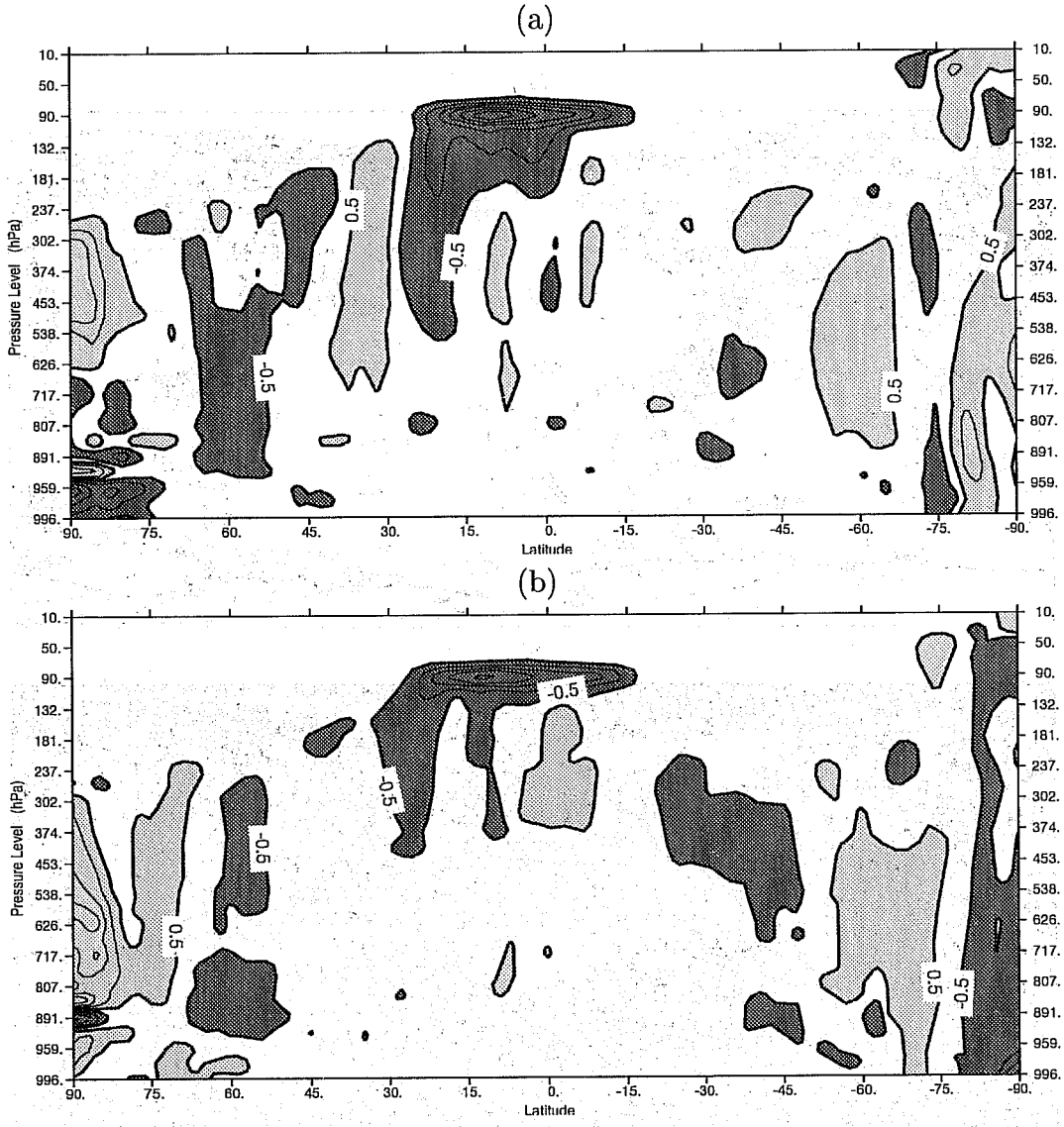

Figure 6: Impact of the radiation time-step on cloudiness. Top panel is the difference between the vertical distribution of the zonally averaged cloud cover, in %, with the ECMWF GCM using NeuroFlux and a radiation time-step of either three hours or one hour (version with three hours minus version with one hour). Contours every 1%; negative values less than -0.5% are dark-shaded, positive values greater than 0.5% are light-shaded.

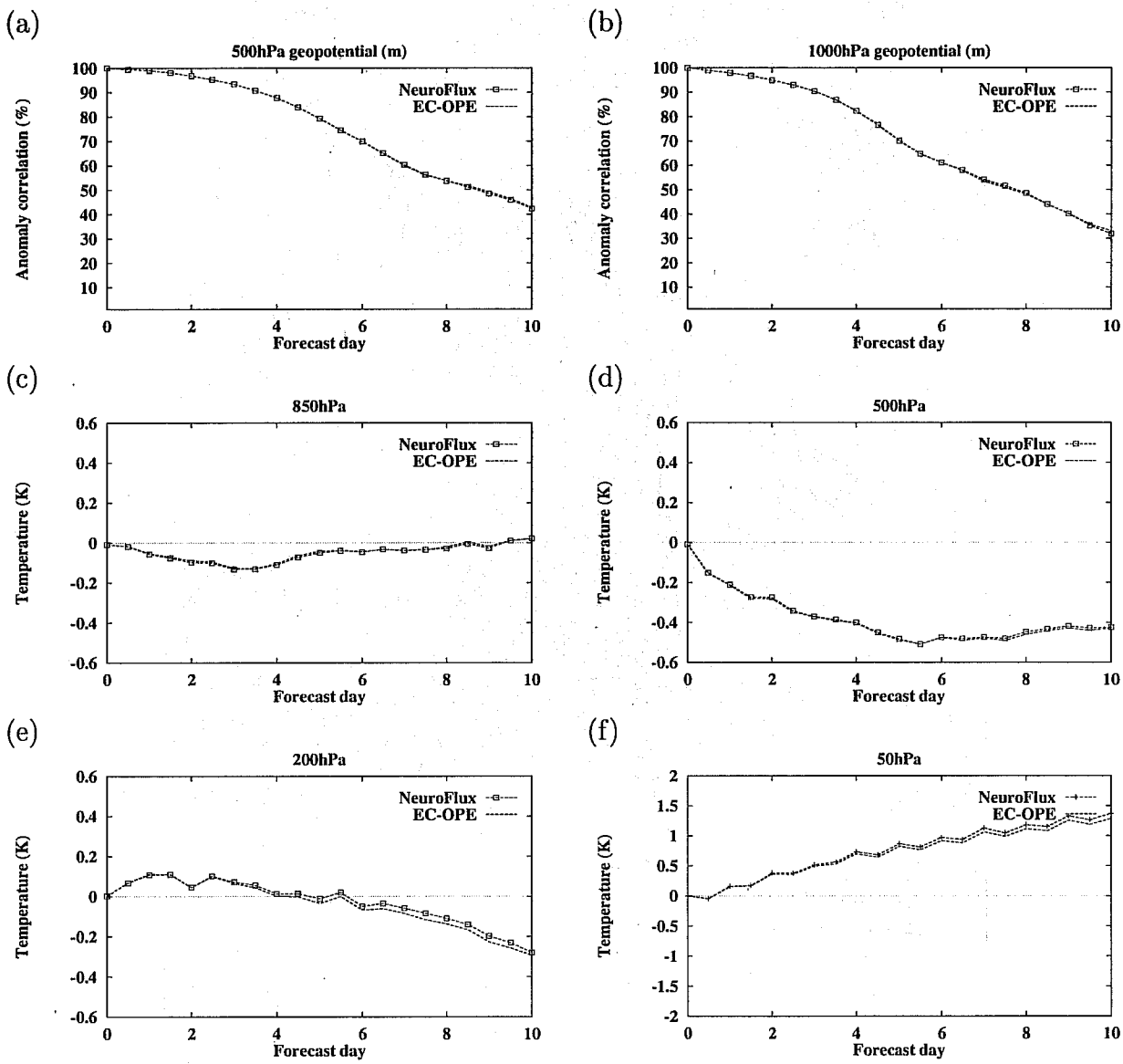

Figure 7: T213 L31 simulations: forecast verification for Northern Hemisphere's geopotential (a,b) and temperature (c,d,e,f). Mean over 12 cases.

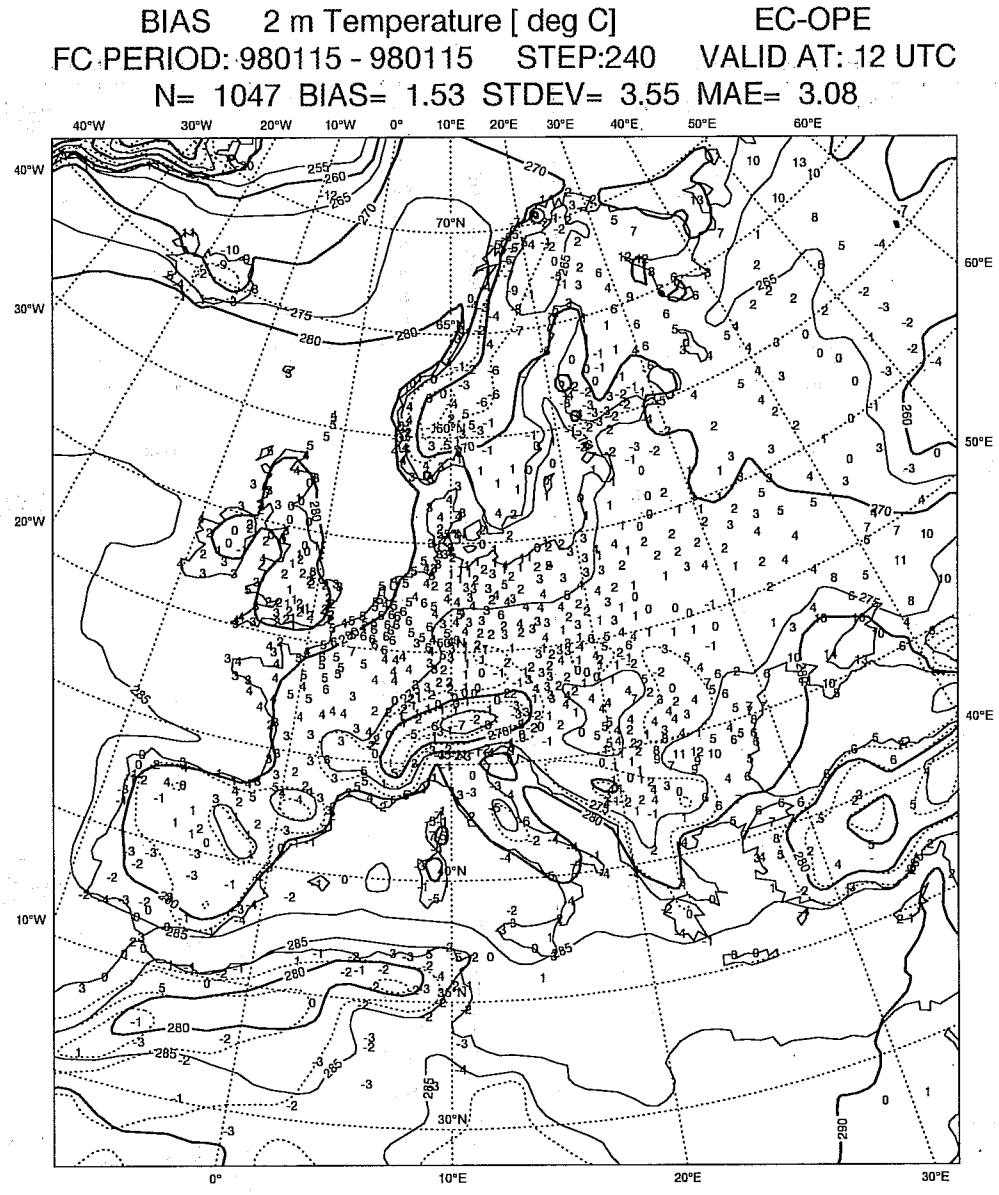

Figure 8: 10-day forecast for 25/01/95 using EC-OPE. Validation of the 2-meter temperature forecast with observations.

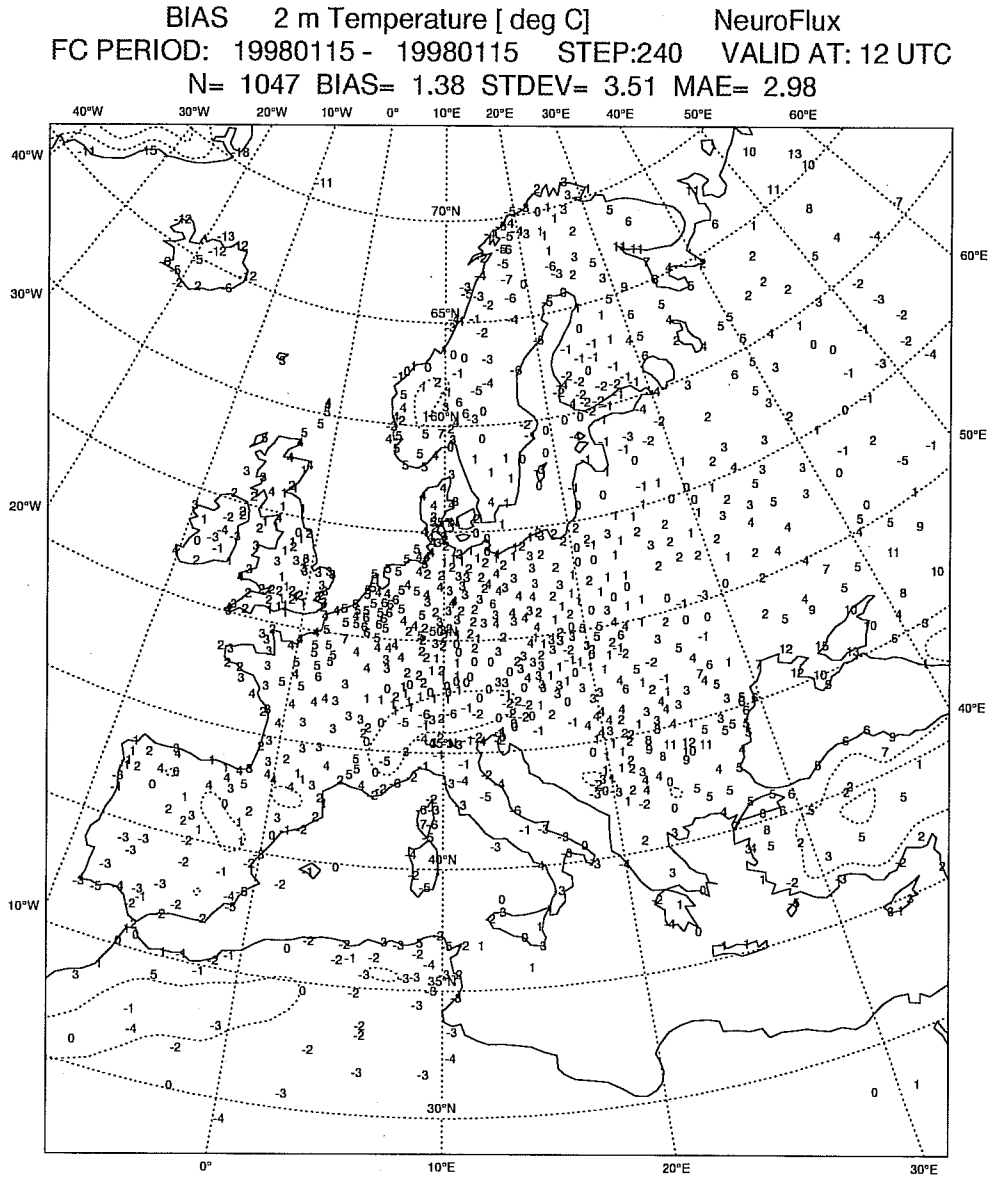

Figure 9: As on figure 8, but with NeuroFlux.